Novel full-duplex SSB WDM-RoF system with SLM technique for decreasing PAPR*

XIAO Yao-qiang (肖要强)**, **CHEN Lin** (陈林), **LI Fan** (李凡), **and HE Hai-zhen** (何海珍)
Key Laboratory for Micro-/Nano-Optoelectronic Devices of Ministry of Education, College of Information Science and Engineering, Hunan University, Changsha 410082, China

(Received 18 March 2013)

A novel full-duplex single-sideband (SSB) wavelength division multiplexing radio over fiber (WDM-RoF) system with selected mapping (SLM) technique for decreasing peak-to-average power ratio (PAPR) is proposed in this paper. At the central office (CO), the generated SSB signal carrying 10 Gbit/s 16-ary quadrature amplitude modulation orthogonal frequency division multiplexing (16QAM-OFDM) downstream signal with SLM technique is sent to the base station, and 60 GHz SSB optical signal carrying 10 Gbit/s 16QAM-OFDM upstream signal is sent back to CO utilizing the wavelength-reuse technology. Simulation results show the proposed method for PAPR reduction can effectively improve the sensitivity of receiver, and the power penalty of the 16QAM-OFDM downlink (uplink) signal is about 2 dB (3 dB) at BER of 1×10^{-3} after 42 km standard single-mode fiber (SSMF) transmission.

Document code: A **Article ID:** 1673-1905(2013)04-0309-4
DOI 10.1007/s11801-013-3050-2

Radio-over-fiber (RoF) technology has attracted much attention for increasing the capacity and mobility of high-speed wireless data transmission[1-4]. Orthogonal frequency division multiplexing (OFDM)[5-7] is widely used in broadband wired and wireless communication systems. Although OFDM has many advantages, the high peak-to-average power ratio (PAPR) is its major drawback[8]. For wavelength division multiplexing (WDM) system, in particular, the output erbium-doped optical fiber amplifier (EDFA) of the transmitter must keep linear over a wide range of signal levels, which makes this kind of EDFA with high cost and power-consumption[9]. To solve the PAPR problem, people have proposed many methods[10-12]. Shao et al[13] have proposed and experimentally demonstrated a simplified full-duplex 60 GHz optical millimeter wave (mm-wave) access system with a 16QAM-OFDM downlink signal generated by selected mapping (SLM). However, in that paper, there are some drawbacks[14].

To improve the performance of system, we propose a novel full-duplex single-sideband (SSB) WDM-RoF system for decreasing PAPR using SLM technique. Theoretical analysis and numerical simulation results indicate that the RoF link architecture shows good performance and can be a promising choice for practical application.

Fig.1 shows the block diagram of OFDM modulation with SLM technique. The input data of the SLM block is a vector of $\boldsymbol{X}=[X_0,X_1,\cdots,X_{N-1}]^{\mathrm{T}}$, where N is the length of $\boldsymbol{X}$ and is equal to the number of sub-carriers. Each of the elements of $\boldsymbol{X}$ represents the data to be carried on the corresponding sub-carrier. In the transmitter with SLM technique, K alternative input symbol sequences $\boldsymbol{S}^{(i)}$ $(1\le i\le K)$ are generated by the component-wise product of the input symbol sequence $\boldsymbol{X}$ and K phase sequences $\boldsymbol{p}^{(i)}=[a_0^{(i)},a_1^{(i)},\cdots,a_{N-1}^{(i)}]^{\mathrm{T}}$ $(1\le i\le K)$. Therefore,

$$\boldsymbol{S}^{(i)}=\boldsymbol{X}\cdot*\boldsymbol{p}^{(i)}=[X_0a_0^{(i)},X_1a_1^{(i)},X_2a_2^{(i)},\cdots,X_{N-2}a_{N-2}^{(i)},X_{N-1}a_{N-1}^{(i)}]^{\mathrm{T}}, \tag{1}$$

where $\cdot*$ denotes the dot product of two vectors, and phase sequences $a_u^{(i)}=\exp(\varphi_u^{(i)})$ $(u=0,\cdots,N-1)$ are the rotation factors. To simplify calculation, we let $a_u^{(i)}$ belong to the set $\{\pm1,\pm j\}$ and select $2\le i\le K$ in $a_u^{(i)}$. After SLM technique, the signal can be expressed as:

$$x_m^{(i)}=\frac{1}{\sqrt{N}}\sum_{k=0}^{N-1}X_ka_k^{(i)}\exp(\mathrm{j}2\pi km/N)\ . \tag{2}$$

When $x_m^{(i)}$ is a band-limited signal with Nyquist frequency, the PAPR of $x_m^{(i)}$ is defined as:

$$PAPR^{(i)}=\frac{\max\limits_{0\le m\le N-1}\left|x_m^{(i)}\right|^2}{E\left[\left|x_m^{(i)}\right|^2\right]}\ . \tag{3}$$

The complementary cumulative distribution function (CCDF) of PAPR is usually used, and can be expressed as

$$\Pr(PAPR>z)=1-(1-\mathrm{e}^{-z})^N\ . \tag{4}$$

* This work has been supported by the National Natural Science Foundation of China (No.60977049), and the National High Technology Research and Development Program of China (No.2011AA010203).
** E-mail: yqxiao6@126.com

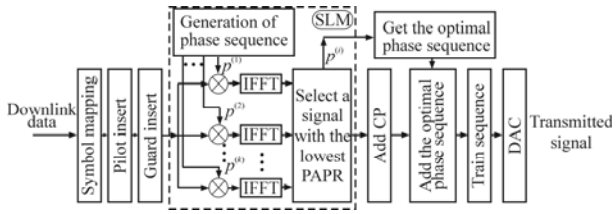

Fig.1 Block diagram of OFDM modulation with SLM technique

After all the K frames of input symbol sequences $\boldsymbol{S}^{(i)}$ are transformed into the time domain signals using inverse fast Fourier transform (IFFT), the signal with minimum PAPR chosen from the K time domain signals is transmitted. In order to recover data, the optimal phase sequence $\boldsymbol{p}^{(i)}$ must also be transmitted to receiver along with the OFDM signal.

Fig.2 shows the block diagram of the novel full-duplex SSB WDM-RoF system with SLM technique for decreasing PAPR. In the central office (CO), the OFDM signal ($x_m(t)=I(t)+\mathrm{j}\cdot Q(t)$) and the electrical RF carriers ($V_I(t)=V_{RF}(t)\cos\omega_{RF}t$, $V_Q(t)=V_{RF}(t)\sin\omega_{RF}t$) are sent to one in-phase and quadrature (I/Q) modulator. Assuming G is the parameter gain, the output mixed signal of I/Q modulator can be expressed as:

$$V_1(t)=G[I(t)V_{RF}\cos(4\omega_{RF}t)-Q(t)V_{RF}\sin(4\omega_{RF}t)]. \quad (5)$$

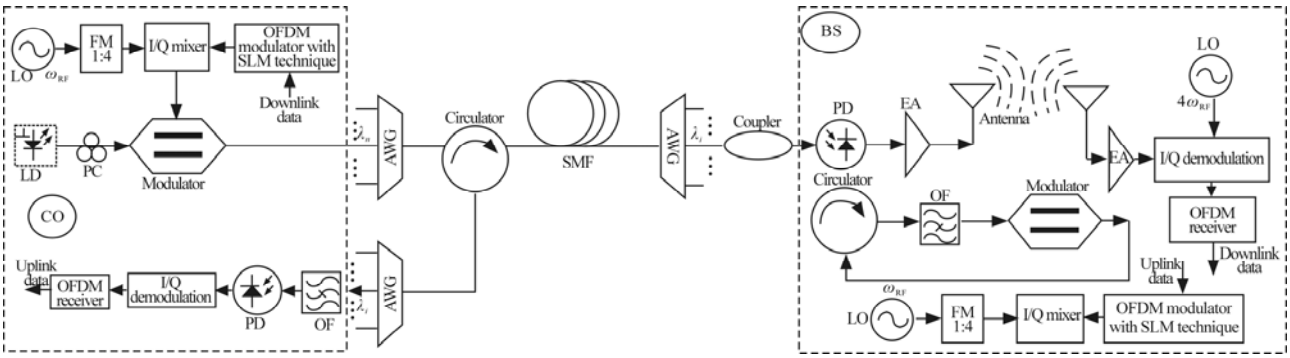

LD: laser diode; MZM: Mach-Zehnder modulator; LO: local oscillator; PC: polarization controller; AWG: array waveguide grating; FM: frequency multiplier; OF: optical filter; PD: photodetector; EA: electrical amplifier

Fig.2 Block diagram of the novel full-duplex SSB WDM-RoF system

When the MZM is biased at $V_\pi/2$, where V_π is the switching voltage of MZM, and a 90° difference is introduced between the mixed electrical voltages $V_1(t)$ and $V_2(t)$, the output of the MZM can be expressed as:

$$E_2(t)\approx\alpha\sqrt{P_0}[\sqrt{2}J_0(m)\mathrm{e}^{\mathrm{j}(\omega_0 t+\pi/4)}+2J_1(m)x_m(t)\mathrm{e}^{\mathrm{j}[(\omega_0+4\omega_{RF})t+\pi/2]}], \quad (6)$$

where α is the insertion loss of the MZM, $m=\pi V_1(t)/V_\pi$ is the modulation index, and $J_n(m)$ is the nth-order Bessel function of the first kind. The optical SSB mm-wave is generated for the downlink. After combining signals of all channels with an arrayed waveguide grating (AWG), the WDM-RoF combining signals are transmitted to base station (BS) along the downlink standard single-mode fiber (SSMF)-28.

After a z km-length SSMF-28, the received optical electrical field in the BS can be written as:

$$E_3(z,t)=\alpha\sqrt{P_0}\mathrm{e}^{-\kappa z/2}\{\lambda_1 J_0(m)\mathrm{e}^{\mathrm{j}[\omega_0 t-\beta(\omega_0)z]}+2\lambda_2 J_1(m)V_1[t-\frac{\beta(\omega_0+4\omega_{RF})}{\omega_0+4\omega_{RF}}z]\times\mathrm{e}^{\mathrm{j}[(\omega_0+4\omega_{RF})t-\beta(\omega_0+4\omega_{RF})z+\delta]}\}, \quad (7)$$

where κ is the optical power attenuation along the fiber, δ is the introduced random phase noise, and $\beta(\omega)$ is the propagation constant of the lightwave at an angular frequency of ω[15]. The optical mm-wave is divided into two parts by a 3 dB optical coupler. One part is delivered to a PIN photodiode to be converted to electrical signal. We assume that only the optical field amplitude is affected in effective bandwidth in such process, and fiber dispersion and nonlinear response have little effect, so the photocurrent can be expressed as:

$$I_1(t)=R_{PIN}\alpha^2P_0\mathrm{e}^{-\kappa z}\{\lambda_1^2J_0^2(m)+4\lambda_2^2J_1^2(m)|V_1[t-\frac{\beta(\omega_0+4\omega_{RF})}{\omega_0+4\omega_{RF}}z]|^2+2\lambda_1\lambda_2J_1(m)J_0(m)V_1[t-\frac{\beta(\omega_0+4\omega_{RF})}{\omega_0+4\omega_{RF}}z]\times\cos[4\omega_{RF}t-4\omega_{RF}\beta'(\omega_0')z+\delta]\}, \quad (8)$$

where R_{PIN} is the responsivity of PIN, $\omega_0'=\omega_0+4\omega_{RF}/2$, and $\beta'(\omega_0')\approx[\beta(\omega_0)-\beta(\omega_0+4\omega_{RF})]/4\omega_{RF}$. After an electrical amplifier with $4\omega_{RF}$ bandwidth, the mm-wave signal is expressed as:

$$I_{\omega_{4RF}}(t)\propto V_1[t-\frac{\beta(\omega_h)}{\omega_h}z]\times\cos[4\omega_{RF}t-4\omega_{RF}\beta'(\omega_h')z+\delta]. \quad (9)$$

The other part is prepared for uplink, and a circulator is used to get the central lightwave at an angular frequency of ω_0 for wavelength-reusing at the BS.

To prove the feasibility of the model above, the simulation architecture of the proposed full-duplex SSB WDM-RoF system with SLM technique for decreasing PAPR is demonstrated in Fig.3. In this paper, the number of subcarriers is 128, and the size of IFFT is 256. The length of the cyclic prefix (CP) is 1/16 of the symbol period. To estimate channel and synchronize time, a training sequence is inserted every 100 symbols, and the FEC overhead is set to 7%.

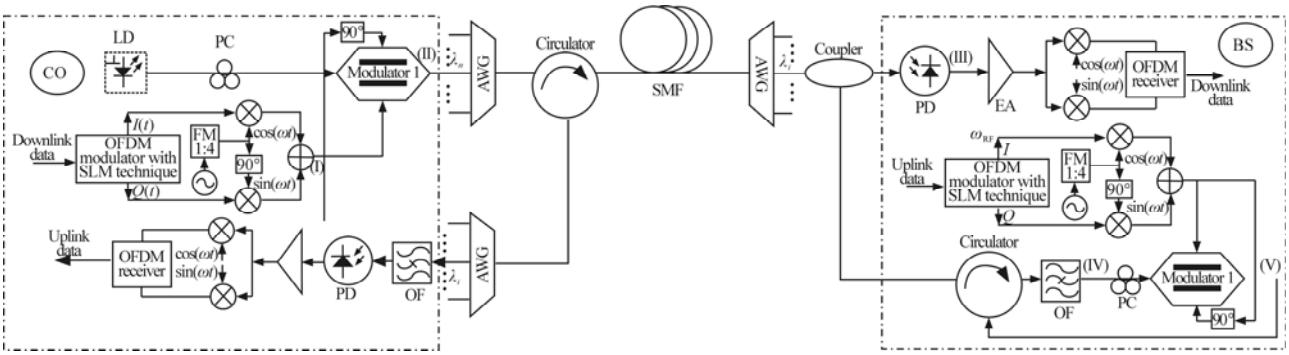

Fig.3 The simulation architecture of full-duplex SSB WDM-RoF system

The CCDF curves of the PAPR with SLM technique for K(=2, 4, 8, 16) branches and without SLM technique are shown in Fig.4. From Fig.4, 16QAM-OFDM signals with SLM for K=16 have significant reduction in PAPR, so SLM technique with K=16 branches (SLM-16) is chosen in this paper.

The generated 16QAM-OFDM signal is mixed with a 60 GHz sinusoidal wave by one I/Q mixer. The mixed signal is used to drive the dual-arm $LiNbO_3$ (LN)-MZM, and the modulated electrical signals of the two arms have a phase shift of 90°. We must carefully adjust the power of RF OFDM signal to maintain a certain power ratio between local oscillator (LO) and the first-order sidebands, while suppressing the second-order modes resulting from the nonlinearity of the modulation to increase dispersion tolerance and receiver sensitivity. The MZM is biased at $V_\pi/2$=2 V, and the optical spectrum of the output of the MZM is shown in Fig.5(b). From Fig.5(b), we can clearly see the output of the MZM mainly consists of the optical carrier at 193.1 THz and the first-order upper-sideband at 193.16 THz.

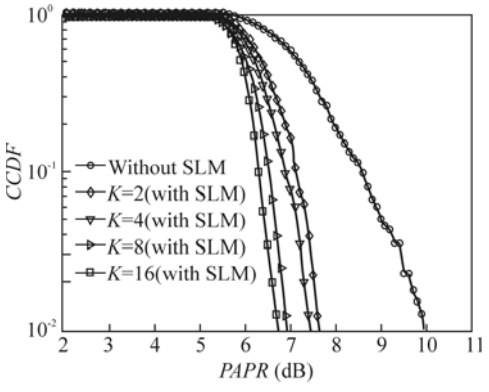

Fig.4 CCDF curves of PAPR

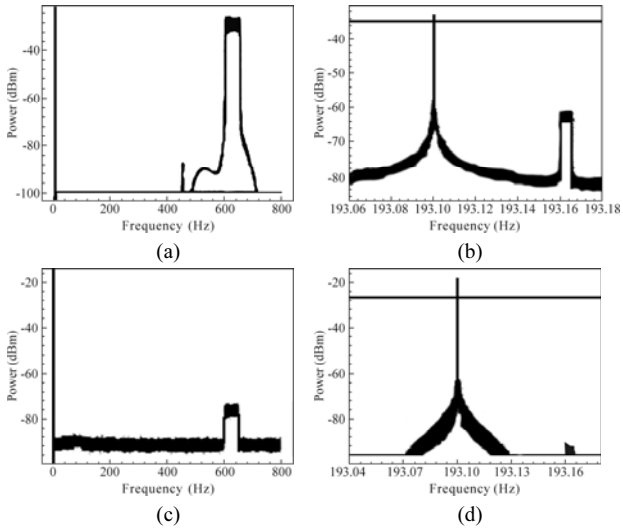

Fig.5 (a) Frequency spectrum of the transmitted 16 QAM-OFDM signal for downlink; (b) Optical spectrum for downlink signal; (c) Electrical spectrum of 60 GHz mm-wave signal; (d) Optical spectrum of the central lightwave for reusing

After the 42 km SSMF-28, an AWG is used as optical demultiplexer to separate optical signals and deliver them to BSs, and the received optical mm-wave is divided into two parts by a 3 dB optical coupler. One part is sent to a PIN receiver with a 3 dB bandwidth of 60 GHz to beat mm-wave signal, whose electrical spectrum is shown in Fig.5(c). It's obvious that the spectrum of the photocurrent mainly includes the 60 GHz mm-wave signal, which is in accord with Eq.(8). After the converted electrical signal is amplified by one RF amplifier with the center frequency of 60 GHz and the bandwidth of 10 GHz, we use the electrical LO signal and an electrical mixer to down-convert the electrical signal. After the OFDM baseband signal passes a low pass filter (LPF), the

downlink data can be recovered through an OFDM receiver.

For uplink, the other part of received optical signal is used to separate the central optical carrier for a cost-effective BS which does not require any local laser. The optical signal is sent to an OF with the center wavelength at 1552.52 nm and bandwidth of 0.1 nm to get the central lightwave for reusing, and the optical spectrum of the central lightwave for reusing is shown in Fig.5(d). The uplink 16QAM-OFDM signal is modulated onto the reused central lightwave via one dual-arm LN-MZM. Because the additional light source is not necessary, and no wavelength management function is required at the BS, the cost is significantly reduced and the stability of system is improved. After the 42 km-length of SSMF-28, the optical mm-wave uplink signal is transmitted back to CO. In the CO, a low-noise EDFA with gain of 30 dB is used to amplify the received optical signal, and then the amplified optical signal is sent to PIN to be converted to electrical domain signal. After the electrical mm-wave signal is demodulated orthogonally, the 16QAM-OFDM signal of uplink is detected and sent to an OFDM receiver for recovering uplink data.

Fig.6 depicts the bit error rate (BER) curves for downlink and uplink with SLM-16 and without SLM before and after 42 km SSMF. After 42 km SSMF-28, the receiver sensitivity with SLM-16 technique for downlink is about -17 dBm at a BER of 10^{-3}, but that without SLM-16 technique is about -16.5 dBm. As for uplink, the receiver sensitivity is about -15.5 dBm with SLM-16 technique, but that is about -15 dBm without SLM technique. From the measurements, we can see the power budget for both downlink and uplink is about 1.5 dB. After 42 km transmission without any optical dispersion compensation, the power penalty of the 16QAM-OFDM downstream signal is about 2 dB at BER of 1×10^{-3}, and for uplink, the power penalty is approximately 3 dB at BER of 1×10^{-3}.

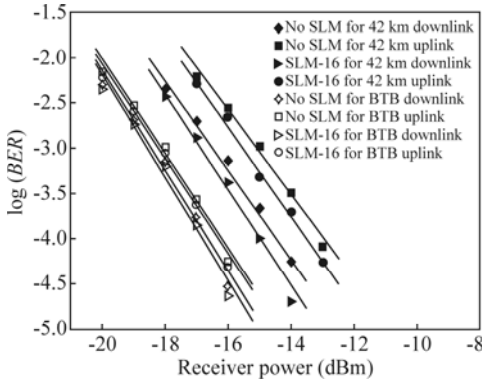

Fig.6 BER curves with and without SLM-16 technique

We propose and demonstrate a novel WDM-RoF architecture with 60 GHz mm-wave SSB links, in which 10 Gbit/s 16QAM-OFDM signals for downlink and uplink are generated with SLM-16 scheme. In this paper, the system is compact and easy to be installed and maintained, because the lightwave source can be reused for uplink. What's more, we don't need an expensive electrical phase shifter to match the RF phase information, which not only makes the adjustment of system to be relatively easy, but also reduces the cost of system. Results show the performance of system can be effectively improved, and the full-duplex WDM-RoF link with proposed SLM scheme may be a feasible architecture in WDM-RoF system.

References

[1] A. Urzdowska and Y. Yashchyshyn, A Full-Duplex Photonic RAU for RoF Systems, Proceedings of European Wireless, 1 (2011).

[2] Y. T. Hsueh, M. F. Huang, S. H. Fan and G. K. Chang, IEEE Photon. Technol. Lett. **23**, 1085 (2011).

[3] C. Taraprasad., Optoelectronics Letters **8**, 293 (2012).

[4] L. Chen, Y. F. Shao, X. Y. Lei, H. Wen and S. C. Wen, IEEE Photon. Technol. Lett. **19**, 387 (2007).

[5] J. Armstrong, J. Lightw. Technol. **27**, 189 (2009).

[6] Z. P. Wang, J. N. Xiao, F. Li and L. Chen, Optoelectronics Letters **7**, 363 (2011).

[7] F. Li, J. J. Yu, J. N. Xiao, Z. Z. Cao and L. Chen, Opt. Commun. **284**, 4699 (2011).

[8] X. Chen, A. Li, G. Gao and W. Shieh, Opt. Express **19**, 26198 (2011).

[9] Y. F. Shao, N. Chi, C. N. Hou, W. L. Fang, J. W. Zhang, B. Huang, X. Y. Li, S. M. Zou, X. Liu, X. Zheng, N. Zhang, Y. Fang, J. B. Zhu, L. Tao and D. X. Huang, J. Lightw. Technol. **28**, 1770 (2010).

[10] L. Wang and C. Tellambura, IEEE Signal Processing Letters **12**, 453 (2005).

[11] S. H. Han and J. H. Lee, IEEE Signal Processing Letters **11**, 887 (2004).

[12] S. Y. Le Goff, S. S. Al-Samahi, Boon Kien Khoo, K. K. Boon, C. C. Tsimenidis and B. S. Sharif, IEEE Transactions on Wireless Communications **8**, 3320 (2009).

[13] Y. F. Shao, N. Chi, J. Y. Fan and W. L. Fang, IEEE Photon. Technol. Lett. **24**, 1301 (2012).

[14] R. P. Braun, G. Grosskopf, D. Rohde and F. Schmidt, IEEE Photon. Technol. Lett. **10**, 728 (1998).

[15] J. X. Ma, Journal of Optical Communications and Networking **3**, 127 (2011).